Limnol. Oceanogr., 58(2), 2013, 533–545
© 2013, by the Association for the Sciences of Limnology and Oceanography, Inc.
doi:10.4319/lo.2013.58.2.0533

Spatial and temporal development of phytoplankton iron stress in relation to bloom dynamics in the high-latitude North Atlantic Ocean

Thomas J. Ryan-Keogh,[a,*] Anna I. Macey,[a] Maria C. Nielsdóttir,[a] Michael I. Lucas,[b] Sebastian S. Steigenberger,[a] Mark C. Stinchcombe,[c] Eric P. Achterberg,[a] Thomas S. Bibby,[a] and C. Mark Moore [a]

[a] Ocean and Earth Science, National Oceanography Centre Southampton, University of Southampton, Waterfront Campus, Southampton, United Kingdom
[b] Marine Research Institute, University of Cape Town, Rondebosch, South Africa
[c] National Oceanography Centre, Southampton, Southampton, United Kingdom

Abstract

The high-latitude North Atlantic (HLNA) is characterized by a marked seasonal phytoplankton bloom, which removes the majority of surface macronutrients. However, incomplete nitrate depletion is frequently observed during summer in the region, potentially reflecting the seasonal development of an iron (Fe) limited phytoplankton community. In order to investigate the seasonal development and spatial extent of iron stress in the HLNA, nutrient addition experiments were performed during the spring (May) and late summer (July and August) of 2010. Grow-out experiments (48–120 h) confirmed the potential for iron limitation in the region. Short-term (24 h) incubations further enabled high spatial coverage and mapping of phytoplankton physiological responses to iron addition. The difference in the apparent maximal photochemical yield of photosystem II (PSII) ($F_v : F_m$) between nutrient (iron) amended and control treatments ($\Delta(F_v : F_m)$) was used as a measure of the relative degree of iron stress. The combined observations indicated variability in the seasonal cycle of iron stress between different regions of the Irminger and Iceland Basins of the HLNA, related to the timing of the annual bloom cycle in contrasting biogeochemical provinces. Phytoplankton iron stress developed during the transition from the prebloom to peak bloom conditions in the HLNA and was more severe for larger cells. Subsequently, iron stress was reduced in regions where macronutrients were depleted following the bloom. Iron availability plays a significant role in the biogeochemistry of the HLNA, potentially lowering the efficiency of one of the strongest biological carbon pumps in the ocean.

The high-latitude ($>\sim 50^{\circ}$N) North Atlantic (HLNA) is characterized by a pronounced spring phytoplankton bloom, representing one of the largest annual productivity cycles in the oceans (Siegel et al. 2002). The associated annual drawdown of macronutrients (e.g., > 10 μmol L^{-1} nitrate) (Sanders et al. 2005) and export production indicate that the biological carbon pump (Volk and Hoffert 1985) of the HLNA is one of the strongest of any large open oceanic region (Laws et al. 2000). Although the annual bloom cycle removes a large proportion of the macronutrients available at the end of winter, further indicating a highly efficient biological carbon pump, residual concentrations of both nitrate and phosphate (e.g., > 1 μmol L^{-1} nitrate) are frequently observed during summer in the region (Sanders et al. 2005; Nielsdóttir et al. 2009).

The large seasonal removal of macronutrients resulting from the North Atlantic spring bloom contrasts strongly with the other high-latitude systems of the subpolar North Pacific and Southern Ocean, which are both characterized by year round high-nitrate, low-chlorophyll (HNLC) conditions, at least partly as a consequence of low iron availability (Boyd et al. 2007). Consequently, despite some early evidence to the contrary (Martin et al. 1993), iron had not been considered to be a potentially limiting micronutrient in the HLNA. However, it was recently demonstrated that summer phytoplankton communities in the Iceland Basin are prone to iron limitation (Nielsdóttir et al. 2009). Consequently, as suggested for the Southern Ocean (Boyd 2002), the dominant bottom-up influences on phytoplankton growth may transition from irradiance during winter to iron during summer in the HLNA. From the perspective of limits on biomass formation (Cullen 1991), such observations are consistent with the relative input ratios of iron and nitrate being lower than phytoplankton requirements at higher latitudes in the North Atlantic (Measures et al. 2008; Nielsdóttir et al. 2009), partly due to low atmospheric iron supply (Jickells et al. 2005; Moore et al. 2006), at least in regions removed from potentially significant local sources (Prospero et al. 2012).

Top-down factors may also influence accumulation of phytoplankton biomass and nutrient drawdown (Walsh 1976; Banse 2002). In addition to a proposed role of predator–prey dynamics during bloom initiation (Behrenfeld 2010), zooplankton grazing (Walsh 1976), which may be particularly high for small phytoplankton groups, likely plays a major role in the subsequent progression and termination of the bloom (Banse 2002). Silicate limitation of large diatoms, which may otherwise have been able to escape grazing control (Cullen 1991), has also been hypothesized to contribute to incomplete nutrient drawdown in the HLNA (Henson et al. 2006). Rather than

* Corresponding author: T.Ryan-Keogh@noc.soton.ac.uk

acting alone, within the classical HNLC regions these mechanisms likely interact with iron stress in maintaining residual macronutrients (Cullen 1991; Price et al. 1994).

Beyond the available evidence for a limited region of the Iceland Basin during summer (Nielsdóttir et al. 2009), the seasonal and spatial extent of any potential iron stress in the HLNA remains poorly resolved. Consequently, the effect of iron availability on the large-scale biogeochemistry of the region is currently difficult to assess. In this study, changes in phytoplankton standing stocks and photophysiology were assessed in both 48–120 h grow-out experiments and high spatial resolution short-term (24 h) incubations in order to investigate the response of natural populations to the relief of potential nutrient stress.

The apparent maximal photochemical yield of photosystem II (PSII) as measured using variable chlorophyll fluorescence ($F_v : F_m$) is particularly sensitive to iron stress, and hence variability in this parameter can provide a powerful diagnostic for investigating iron stress in the field (Kolber et al. 1994; Boyd and Abraham 2001; Behrenfeld et al. 2006). The value of $F_v : F_m$ is frequently observed to be suppressed within HNLC systems and, more significantly, increases rapidly following iron resupply to iron-stressed field populations both in situ (Kolber et al. 1994; Boyd and Abraham 2001) and in bottle incubations (Greene et al. 1994; Moore et al. 2007; Nielsdóttir et al. 2009). Measurement of such rapid photophysiological changes following deliberate experimental manipulations avoids potential problems in the interpretation of, for example, the absolute value of $F_v : F_m$ in situ, where any physiological signal will be superposed over taxonomic variability (Suggett et al. 2009). In addition, because physiological changes will precede resultant changes in biomass accumulation, restricting experimental time when monitoring sensitive changes to the photosynthetic apparatus minimizes the influence of bottle effects on biomass accumulation and the potential confounding influence of shifts in community structure on physiological measurements (Geider and La Roche 1994; Greene et al. 1994).

The current study thus aimed to establish the seasonal cycle of iron stress across both the Iceland and Irminger Basins of the HLNA. By combining in vitro incubation experiments with remote sensing data and in situ measurements of phytoplankton physiology, macronutrients, and chlorophyll, we mapped the development of physiological iron stress. Moreover, contrasting responses to iron addition observed in different biogeographical regions allowed us to describe the seasonal progression of iron stress within the HLNA and assess the potential for both iron limitation of phytoplankton growth and macronutrient removal.

Methods

Data were obtained during two cruises of the RRS *Discovery* to the HLNA, a spring cruise (D350) from 28 April to 10 May 2010 (Day of Year (DOY) 118–130) and a summer cruise (D354) from 04 July to 10 August 2010 (DOY 185–222). During the spring cruise eight short-term (24 h) and two long-term (> 24 h) incubation experiments were performed. A further 17 short-term and 7 long-term incubation experiments were undertaken during the summer cruise. Trace metal clean water for the incubation experiments was pumped from a trace metal clean fish towed at a depth of ~ 4 m, while the ship was steaming at no less than 5 knots, into a dedicated clean chemistry container using a polytetrafluoroethylene diaphragm pump (Almatec 15).

Incubation experiments were performed using similar methods to those employed previously in the HNLC Southern Ocean and Iceland basin (Moore et al. 2007; Nielsdóttir et al. 2009). Water for the experiments was collected and transferred unscreened into acid-washed 1 liter polycarbonate bottles (Nalgene) for the 24 h incubation experiments and 4.5 liter polycarbonate bottles for the long-term incubation experiments. All water was collected during the hours of darkness. Incubation bottles were filled in a random order with the triplicate samples for initial measurements collected at the beginning, middle, and end of the filling process. In addition to an unamended control, within the 24 h incubation experiments, different treatments were amended with 0.2 nmol L^{-1} $FeCl_3$, 2.0 nmol L^{-1} $FeCl_3$, 1.0 μmol L^{-1} NO_3^-, or 2.0 nmol L^{-1} $FeCl_3$ and 1.0 μmol L^{-1} NO_3^- (hereafter, + 0.2 Fe, + 2.0 Fe, + 1.0 N and + FeN); all experimental conditions were conducted as biological duplicates or triplicates.

Long-term experiments were run for 48–120 h and consisted of two treatments, a control and 2.0 nmol L^{-1} Fe addition only (hereafter, + Fe), or four treatments, a control, 2.0 nmol L^{-1} Fe, 1.0 μmol L^{-1} NO_3^- and 2.0 nmol L^{-1} Fe + 1.0 μmol L^{-1} NO_3^- (hereafter, + Fe, + N, and + FeN). All bottle tops were sealed with film (Parafilm™), and bottles were double bagged with clear plastic bags to minimize contamination risks on deck. On-deck incubations were performed using "blue lagoon" filters (LEE Filters) to provide light levels corresponding to 35% of above surface irradiance. Running surface seawater was used to control the temperature in the incubators.

Samples for analysis of chlorophyll and macronutrients were collected from both the experiments and from the ship's nontoxic underway seawater supply, which has an intake depth of ~ 5 m. Samples for chlorophyll analysis (250 mL) were filtered onto GF/F or 5 μm polycarbonate filters (Whatman) and then extracted into 90% acetone for 24 h in the dark at 5°C before analysis with a fluorometer (TD70; Turner Designs) (Welschmeyer 1994). Macronutrient samples were drawn into 40 mL diluvials and immediately refrigerated at 4°C until analysis, which typically commenced within 12 h of sampling. A subset of macronutrient samples was filtered and frozen for post-cruise analysis. Concentrations of the macronutrients nitrate plus nitrite (hereafter dissolved inorganic nitrogen [DIN]), phosphate, and silicate were determined using a Skalar San Plus autoanalyzer as described previously (Sanders and Jickells 2000). Concentrations of dissolved iron for samples collected using the trace metal clean fish were determined by isotope dilution inductively coupled plasma mass spectrometry as described by Milne et al. (2010). Analysis was performed on an Element II instrument (ThermoFisher Scientific, Bremen, Germany)

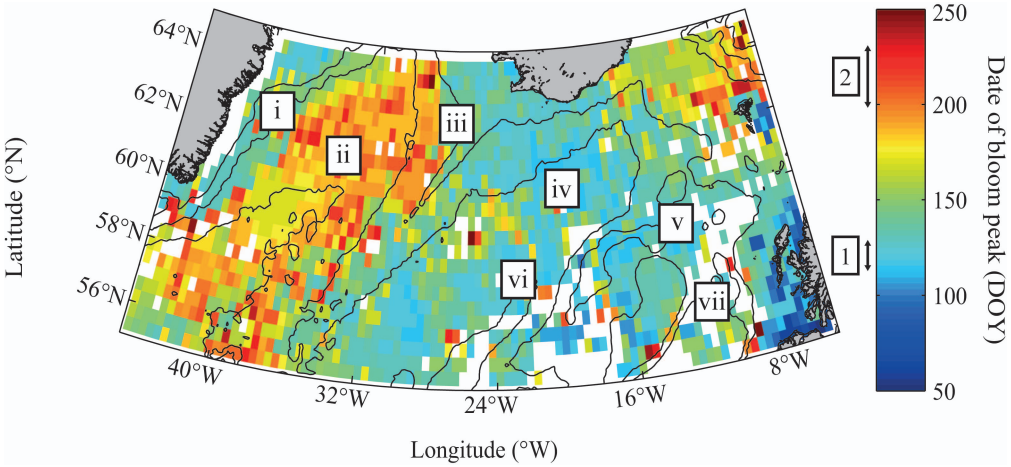

Fig. 1. Date of bloom peak for the HLNA calculated using MODIS data. Black contours correspond to bathymetry in 1000 m isobaths. Indicated on colorbar are approximate timings of both cruises, where 1 = D350 (spring) and 2 = D354 (summer). Geographic regions of the HLNA include i = Western Irminger Basin, ii = Central Irminger Basin, iii = Reykjanes Ridge, iv = Iceland Basin, v = Rockhall Bank, vi = Hatton Bank, and vii = Rockhall Trough.

following an offline preconcentration and matrix removal step via solid phase extraction on a column filled with the chelating resin Wako carboxymethylated pentaethylene-hexamine (CM-PEHA). Accuracy of the method was verified by analysing 'sampling and analysis of iron reference (SAFE)' samples.

Chlorophyll fluorescence measurements for discrete water samples were performed using a Chelsea Scientific Instruments Fasttracka™ Mk II Fast Repetition Rate fluorometer (FRRf) integrated with a FastAct™ Laboratory system. Subsampling of incubations for chlorophyll, macronutrient concentrations, and FRRf occurred between 00:00 and 03:00 local time. All samples were dark acclimated for 30 min, and FRRf measurements were corrected for the blank effect using carefully prepared 0.2 μm filtrates for all experiments and time points (Cullen and Davis 2003). Blanks were typically around 1% and always $<$ 10% of the maximal fluorescence signal. Size-fractionated FRRf measurements were performed by gentle filtration through a 5 μm polycarbonate filter, with the $<$ 5 μm fraction measured directly on the filtrate and the $>$ 5 μm fraction measured following gentle resuspension of retained cells in 0.2 μm filtered seawater. Fluorescence was also recorded underway using a Chelsea Scientific Instruments Fasttracka™ Mk I FRRf. Protocols for FRRf measurements and data processing were similar to those detailed elsewhere (Moore et al. 2007).

Satellite ocean color data were used to place in situ and experimental data within the context of the annual spring bloom cycle. Moderate Resolution Imaging Spectroradiometer (MODIS) 8 day composites were first used to generate a 40 day running mean 0.42 degree, 8 day resolution time series of surface chlorophyll for 2010. The date of the bloom peak was then pragmatically identified at each location as the first time at which the rate of change of the net chlorophyll growth rate dropped below 8×10^{-4} d^{-2}, provided the bloom had already reached $>$ 0.7 μg Chl L^{-1}. Visual inspection of the satellite chlorophyll time series and comparison with in situ data (*see* below) confirmed that this criterion was a reasonable predictor of the early stage of the bloom peak in the region.

Results

Satellite data were used to derive the timing of the spring bloom in both the Iceland and Irminger Basins of the HLNA during 2010 (Fig. 1). The criterion chosen to identify the date of the peak indicated a later bloom in the Central Irminger Basin than elsewhere in the region (Fig. 1). This difference in bloom timing during 2010 was confirmed by in situ measurements of chlorophyll and macronutrients. In situ chlorophyll concentrations peaked during the spring cruise in the Iceland Basin (Fig. 2a) and the summer cruise in the Central Irminger Basin (Fig. 2b). Overall, the transition from spring to summer in the Iceland Basin corresponded to a decrease in average in situ chlorophyll concentrations from $\sim$ 2 to $\sim$ 1.5 μg L^{-1}, compared with an increase from $\sim$ 1.0 to $\sim$ 2.5 μg L^{-1} in the Central Irminger Basin. Alongside these changes in chlorophyll concentration, there were marked decreases in the in situ DIN (Fig. 2c,d) and silicate (Fig. 2e,f) concentrations from spring to summer, with the Iceland Basin having lower concentrations than the Irminger Basin for both seasons. In particular, summer DIN concentrations in the central Iceland Basin were $<$ 1 μmol L^{-1} (Fig. 2d), with silicate $<$ 0.3 μmol L^{-1} (Fig. 2f). Initial dissolved ($<$ 0.4 μm) iron concentrations at experimental locations were frequently lower in summer, with concentrations measured at more than half the summer stations (range $<$ 0.01–0.28 nmol L^{-1}) being below the minimum values encountered during spring (range 0.07–0.28 nmol L^{-1}).

Sea surface values of in situ $F_v : F_m$, measured during the period of darkness (local midnight $\pm$ 4 h) also displayed marked changes in both basins across the seasons, with generally higher values in spring. Superposed onto this seasonal signal, in situ values of $F_v : F_m$ were higher in the

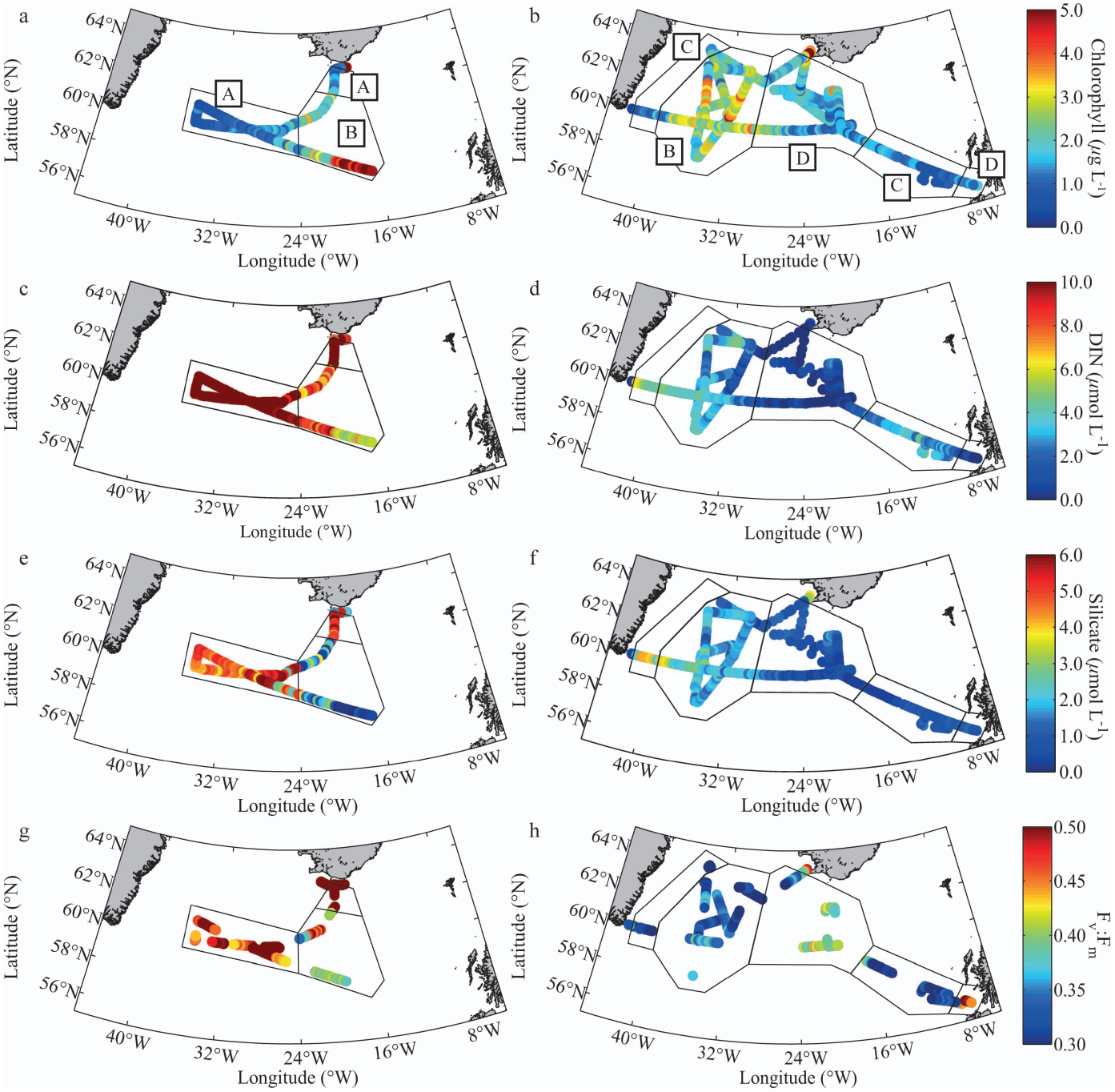

Fig. 2. (a,b) Sea surface chlorophyll concentrations (μg L^{-1}), (c,d) dissolved inorganic nitrogen (DIN) concentrations (μmol L^{-1}), (e,f) silicate concentrations (μmol L^{-1}), and (g,h) nighttime $F_v : F_m$ value during the (a,c,e,g) spring and (b,d,f,h) summer cruises. Solid black lines delineate regions on the basis of in situ sea surface variables and bloom timing during both cruises. (a,b) Regions are labeled according to conditions that correspond to (A) prebloom, (B) bloom, (C) postbloom, high DIN, and (D) postbloom, low DIN.

Irminger Basin than the Iceland Basin in spring (Fig. 2g) but lower in the Irminger Basin and Rockall region than the Iceland Basin in summer (Fig. 2h). By combining these in situ sea surface variables with the bloom timings, different regions of the HLNA could be defined and ascribed to the different bloom stages and conditions during both cruises. Satellite-derived bloom timing was first used to separate the temporal progression of bloom into broad prebloom, bloom, and postbloom periods. Regions and periods sampled under postbloom conditions were then further differentiated on the basis of observed residual macronutrient (DIN) concentrations. Consequently, we identify four broad conditions encountered in different regions over different periods during the two cruises, namely, prebloom (labeled A in Fig. 2), bloom (labeled B), postbloom high DIN (labeled C), and postbloom low

Table 1. Locations for long-term experiments conducted during D350 (spring) and D354 (summer) alongside values of initial and 24 h $F_v:F_m$, and net growth rates estimated from chlorophyll accumulation and nitrate drawdown over the first 72 h (except as noted below). Shown are averages ± standard errors ($n = 2$ or 3).

Cruise	Exp.	Lat. (°N)	Long. (°W)	$F_v:F_{m\ Initial}$	$F_v:F_{m\ Control}$, 24 h	$F_v:F_{m\ Fe}$, 24 h	$\mu^{Chl}_{Control}$ (d^{-1}), 0–72 h	μ^{Chl}_{Fe} (d^{-1}), 0–72 h	$\Delta NO_{3Control}^-$ (μmol L^{-1} d^{-1}), 0–72 h	ΔNO_{3Fe}^- (μmol L^{-1} d^{-1}), 0–72 h
D350	1	60.97	−34.86	0.38±0.02	0.57±0.01	0.58±0.00	0.10±0.02	0.12±0.01	0.18±0.03	0.20±0.03
D350	2	59.99	−29.20	0.48±0.01	0.49±0.01	0.50±0.00	0.11±0.03	0.09±0.00	1.47±0.04	1.52±0.03
D354	1	59.99	−19.91	0.19±0.04	*	*	0.22±0.02†	0.20±0.02†	0.35±0.00†	0.35±0.00†
D354	2	60.00	−20.47	0.36±0.00	0.37±0.01	0.39±0.01	−0.10±0.01†	−0.12±0.01†	0.14±0.00†	0.14±0.00†
D354	3	60.00	−34.38	0.32±0.01	0.26±0.04	0.33±0.01	−0.12±0.14	0.14±0.04	0.13±0.14	0.52±0.19
D354	4	63.03	−35.29	0.29±0.01	0.30±0.01	0.39±0.01	−0.04±0.02	0.25±0.01	0.19±0.04	0.57±0.05
D354	5	58.16	−35.03	0.34±0.00	0.33±0.01	0.39±0.00	0.02±0.01	0.24±0.01	0.18±0.00	0.52±0.02
D354	6	63.84	−34.74	0.29±0.00	0.31±0.00	0.40±0.00	0.04±0.00	0.28±0.01	0.81±0.05	0.76±0.23
D354	7	61.37	−21.16	0.37±0.01	0.36±0.01	0.41±0.01	0.03±0.01	0.15±0.02	0.19±0.01	0.21±0.00

* Measurement not performed.
† In D354 experiments 1 and 2, growth rates and nitrate drawdown were calculated over the first 48 h.

DIN (labeled D). These regions, defined on the basis of in situ observations and satellite-derived bloom timings, subsequently provided context for the analysis of the experimental observations.

Long-term (> 24 h) incubation experiments—Data from 48–120 h experiments indicated variable responses to iron addition to the extant phytoplankton communities (*see* Table 1). During spring, no evidence for iron stress was observed for an experiment initiated over the Reykjanes Ridge (experiment D350.2) (Fig. 3a), with no significant differences in $F_v:F_m$ (analysis of variance [ANOVA], $p > 0.05$) or chlorophyll concentration (Fig. 3b) (ANOVA, $p > 0.05$) observed between the iron addition and control bottles at any time point. During the same season an experiment set up in the Central Irminger Basin (experiment D350.1) provided some evidence that the in situ phytoplankton community had the potential to become iron stressed, with relative decreases in $F_v:F_m$ in the control treatment (Fig. 3c) and increased chlorophyll concentration (Fig. 3d) seen within the iron-addition treatment compared with the control treatment after 120 h of incubation. Enhanced nutrient drawdown (data not shown) after 120 h was also evident within the iron-addition treatment, with nitrate drawdown, calculated as the difference between the initial concentration and the final concentration (ΔNO_3^- (μmol L^{-1} d^{-1})) being significantly higher (ANOVA, $p < 0.05$) at 0.26 ± 0.01 (μmol L^{-1} d^{-1}) in the iron-addition treatment compared with 0.21 ± 0.01 (μmol L^{-1} d^{-1}) for the control treatment.

During the summer, iron addition had a more pronounced influence on phytoplankton community responses, particularly in the Irminger Basin. Rapid increases in $F_v:F_m$ were frequently observed within 24 h of iron amendment, as illustrated by a representative experiment from the Western Irminger Basin (experiment D354.6) (Fig. 3e). These rapid physiological changes were subsequently followed by increased nutrient drawdown and biomass accumulation, as inferred from bulk chlorophyll concentrations (Fig. 3f; Table 1). Net growth rates estimated from increases in chlorophyll and nutrient drawdown following iron addition were frequently higher than that in controls, particularly in the Central and Western Irminger Basin (Table 1).

In contrast, within the Iceland Basin during the summer cruise, where surface nitrate concentrations were frequently undetectable (< 0.03 μmol L^{-1}) (Fig. 2d), no chlorophyll increases were observed on addition of nitrate alone, while the greatest increases in chlorophyll were typically observed only following the combined addition of both iron and nitrate. For example, during experiment D354.7 (Fig. 3h), net chlorophyll based growth rates within the combined (+ FeN) treatment were ~ 80% and 40% higher than observed in controls or iron alone additions, respectively. However, iron addition resulted in the same increase in $F_v:F_m$ as the combined treatment (+ FeN), while $F_v:F_m$ for the nitrate treatment was indistinguishable from the control (Fig. 3g). Consequently, although iron addition alone promoted a rapid photophysiological response (Fig. 3g), significantly higher chlorophyll accumulation within the

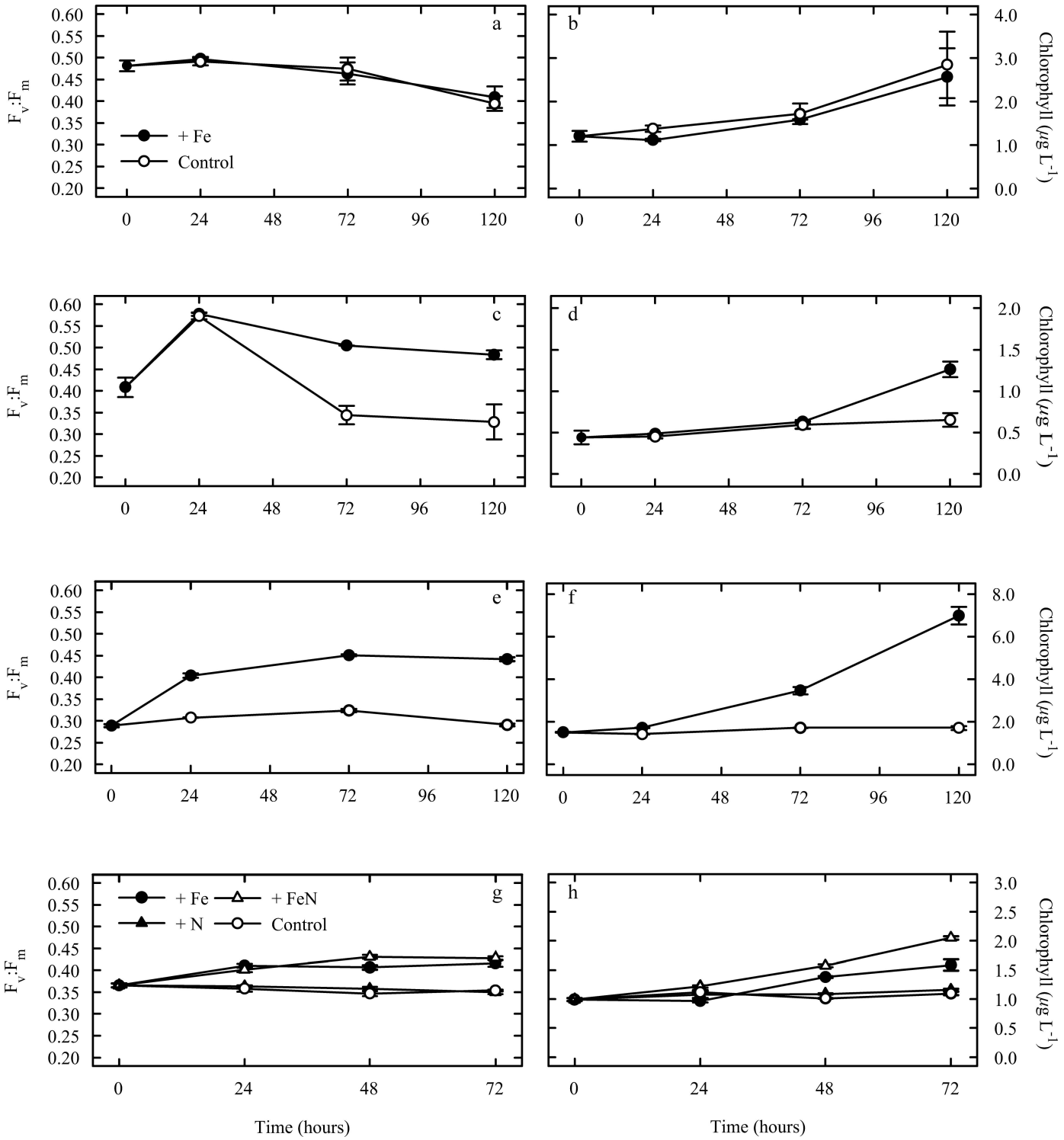

Fig. 3. $F_v : F_m$ and chlorophyll responses (μg L^{-1}) from representative long-term (> 24 h) experiments initiated over (a,b) the Reykjanes ridge (spring) (experiment D350.2), (c,d) the Irminger basin (spring) (experiment D350.1), (e,f) the Irminger basin (summer) (experiment D354.6), and (g,h) the Iceland basin (summer) (experiment D354.7). Shown are averages with ± standard errors, (n = 3 for all time points of the Iceland basin experiment, whereas n = 3, 2, 2, and 5 for time points 0, 24, 72, and 120 h, respectively, in the other experiments).

+ FeN (Fig. 3h) was suggestive of a system approximating a state of iron and nitrate colimitation (Arrigo 2005; Saito et al. 2008).

Short-term (24 h) incubation experiments—The 25 short-term 24 h incubation experiments conducted over both cruises further revealed variability between basins and seasons. Significant (ANOVA, $p < 0.05$) rapid changes in photophysiology ($F_v : F_m$) were often observed in these experiments, despite the lack of significant changes in other variables such as chlorophyll or nutrient concentration over the short 24 h time scale. In order to contrast relative changes in PSII photophysiology between the large numbers of experiments, we calculated the difference in $F_v : F_m$ between control and treatment bottles ($\Delta(F_v : F_m)$). $\Delta(F_v : F_m)$ was calculated for all the different nutrient addition treatments performed during both cruises over the two seasons (Fig. 4). For simplicity, calculated values of $\Delta(F_v : F_m)$ are hereafter subscripted "+ 1.0 N," "+ FeN," "+ 0.2 Fe," or "+ 2 Fe" corresponding to the 1 μmol L^{-1} nitrate, 1 μmol L^{-1} nitrate and 2.0 nmol L^{-1} Fe, 0.2 nmol L^{-1} and 2.0 nmol L^{-1} iron additions, respectively.

Values of $\Delta(F_v : F_m)_{+1.0\ N}$ were frequently indistinguishable from zero (Fig. 4) or slightly negative, due to a small drop in $F_v : F_m$ following N addition in some experiments, as previously observed in some other systems (Behrenfeld et al. 2006). In contrast, $\Delta(F_v : F_m)$ was frequently positive following iron addition (Figs. 4, 5), with the values calculated for the two iron alone treatments (+ 0.2 Fe and + 2.0 Fe) being highly correlated ($r^2 = 0.960$, $n = 23$, $p < 0.001$) and hence displaying consistent spatial patterns (Fig. 5). Moreover, within those natural populations displaying significant responses (ANOVA, $p < 0.05$), the addition of 2.0 nmol L^{-1} iron consistently resulted in a larger change in $F_v : F_m$ (on average 40% higher) than the addition of 0.2 nmol L^{-1} iron (Figs. 4b, 5). Consequently the observed variability of $\Delta(F_v : F_m)$ following iron addition ($\Delta(F_v : F_m)_{+0.2\ Fe\ or\ +2.0\ Fe}$) indicated spatially and temporally coherent physiological responses that scaled with increasing iron enrichment (Fig. 5). We thus interpret $\Delta(F_v : F_m)_{+0.2\ Fe\ or\ +2.0\ Fe}$ as a relative measure of the degree of iron stress, providing a means to compare and contrast the interbasin and intrabasin and seasonal variability.

Values of $\Delta(F_v : F_m)_{+0.2\ Fe\ or\ +2.0\ Fe}$ were lowest under the prebloom conditions (labeled A in Fig. 2), suggesting a lack of physiological iron stress for these populations (Figs. 4a; 5a,b), consistent with the lack of a treatment response in longer term grow-out experiments performed under the same conditions (Fig. 3a). Low $\Delta(F_v : F_m)$ was also observed following iron addition within the postbloom low DIN conditions (labeled D in Fig. 2) encountered in the Iceland Basin (Fig. 5c,d), where the + FeN treatment also tended to have a higher $\Delta(F_v : F_m)$ than that for iron alone (data not shown) and where longer term experiments indicated the potential for colimitation of chlorophyll accumulation by iron and nitrate (Fig. 3h). Higher values of $\Delta(F_v : F_m)_{+0.2\ Fe\ or\ +2.0\ Fe}$ were observed during the bloom conditions (labeled B in Fig. 2) encountered in the Iceland Basin during the spring cruise (Fig. 5a,b) and the Central Irminger Basin during the summer cruise (labeled B in Fig. 2) (Fig. 5c,d), while the highest values were observed under postbloom high DIN conditions (labeled C in Fig. 2), as encountered in the Western Irminger Basin and Rockall region during the summer cruise (Fig. 5c,d). These regions corresponded to the clearest influence of iron addition on chlorophyll accumulation and nitrate drawdown in longer term experiments (Fig. 3f, Table 1).

To provide a more quantitative comparison of short-term ($\leq$24 h) physiological responses to nutrient amendment with longer-term biomass responses inferred from bulk chlorophyll accumulation, we compared the value of $\Delta(F_v : F_m)_{+2.0\ Fe}$ observed after 24 h in the long-term experiments (Table 1) with differences in chlorophyll derived net growth rates over 72 h between iron amended and control treatments (Fig. 6). Values of $\Delta(F_v : F_m)_{+2.0\ Fe}$ and $\Delta\mu^{Chl}$ were highly correlated ($R^2 = 0.87$, $p < 0.05$, $n = 8$) (Fig. 6), indicating that the observed short-term physiological responses were predictive of subsequent biomass responses in experiments.

Size-fractionated photosynthetic physiology—Size-fractionated $F_v : F_m$ measurements performed on the initial samples from incubation experiments, revealed a consistent pattern throughout both basins, with the < 5 μm size fraction having a higher in situ $F_v : F_m$ than the > 5 μm size fraction. Overall, $F_v : F_m$ values for the < 5 μm and > 5 μm fractions were, respectively, $\sim$ 10% higher and $\sim$ 25% lower than those of the bulk community. Although both size classes physiologically responded to the addition of Fe (Fig. 7), the response of the > 5 μm size fraction was generally larger (Fig. 7a). For example, in a longer timescale experiment (experiment D354.6) performed in the Western Irminger Basin, the value of $F_v : F_m$ for the > 5 μm fraction had nearly increased to that of the iron-amended < 5 μm fraction after 120 h (Fig. 7a). The addition of iron also resulted in a net chlorophyll derived growth rate for the > 5 μm fraction (over 120 h) that was double that of the < 5 μm size fraction (0.45 ± 0.01 $\mu^{Chl>5}$ (d^{-1}) compared with 0.22 ± 0.01 $\mu^{Chl<5}$ (d^{-1})) (Fig. 7b). However, within the Iceland Basin, although $F_v : F_m$ was also lower for the > 5 μm size fraction than the < 5 μm size fraction (Fig. 7c), the increase was less pronounced and $F_v : F_{m>5\mu m}$ did not increase to a value equivalent to that of the initial or control < 5 μm size fraction. The chlorophyll concentration in the < 5 μm size fraction also remained higher than that for the > 5 μm size fraction in this experiment (Fig. 7d).

Discussion

The annual cycle of phytoplankton growth in the HLNA results in significant seasonality in surface macronutrient concentrations. During winter, photosynthesis is likely limited by low mean irradiance, with net phytoplankton growth occurring rapidly following the onset of stratification (Sverdrup 1953), although alternative controlling factors have been suggested for bloom initiation (Behrenfeld 2010). Subsequently, in contrast to the majority of high-latitude open ocean systems, where large seasonal macronutrient drawdown appears to be restricted by the

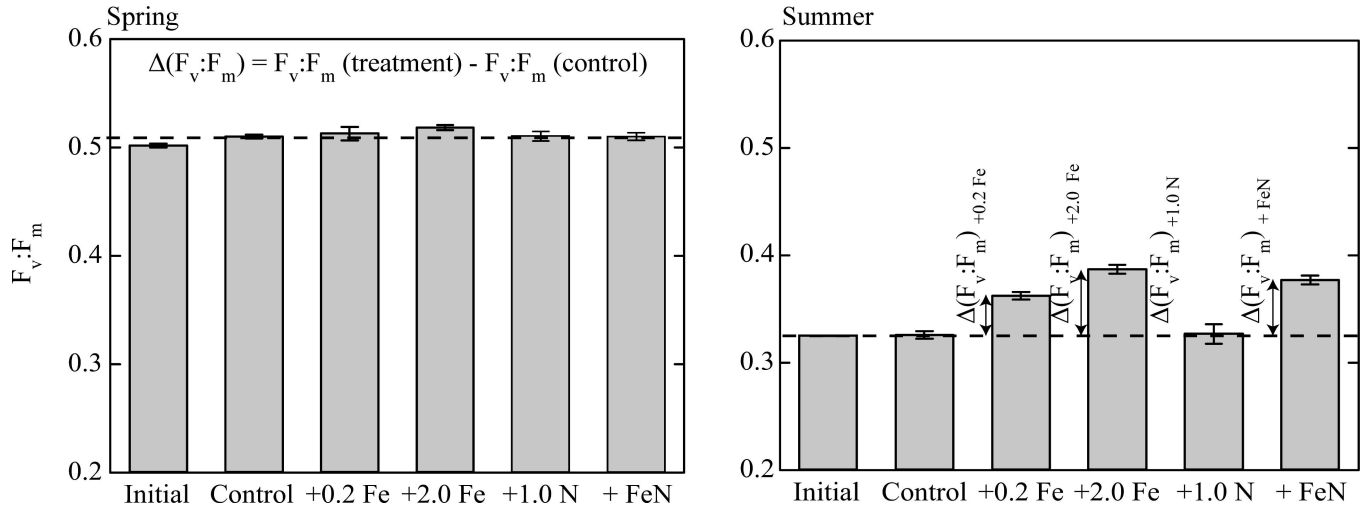

Fig. 4. Representative data from two short-term experiments set up during D350 (spring) and D354 (summer). $\Delta(F_v:F_m)$ is calculated as the difference between the $F_v:F_m$ of the nutrient amended treatment and the control treatment at the 24 h time point. Four different values were calculated, $\Delta(F_v:F_m)_{+0.2\ Fe}$, $\Delta(F_v:F_m)_{+2.0\ Fe}$, $\Delta(F_v:F_m)_{+1.0\ N}$, and $\Delta(F_v:F_m)_{+FeN}$. Dashed line represents level of control treatment. Shown are averages with ± standard errors, where $n = 3$ for all treatments.

availability of iron (Martin and Fitzwater 1988; De Baar et al. 1990; Boyd et al. 2007), macronutrient drawdown over the growing season in the HLNA can be substantial. However, despite the magnitude of the bloom, residual DIN concentrations have frequently been observed in the HLNA at the end of the growing season (Sanders et al. 2005; Nielsdóttir et al. 2009), suggesting that some factor is constraining the complete use of this nutrient resource (Cullen 1991; Greene et al. 1994). Although a lack of bioavailable iron is one possibility (Nielsdóttir et al. 2009), zooplankton grazing (Walsh 1976) or silicate limitation (Henson et al. 2006) could also play a role.

Satellite-derived estimates of bloom timing (Fig. 1) enabled us to place the observed spatial and temporal variability of in situ variables and experimental indices of iron stress within the annual bloom cycle (Fig. 8). In situ observations of chlorophyll and nutrients confirmed the temporal progression of a classical "spring bloom," with macronutrient drawdown accompanying the peak accumulation of phytoplankton biomass, as inferred by bulk

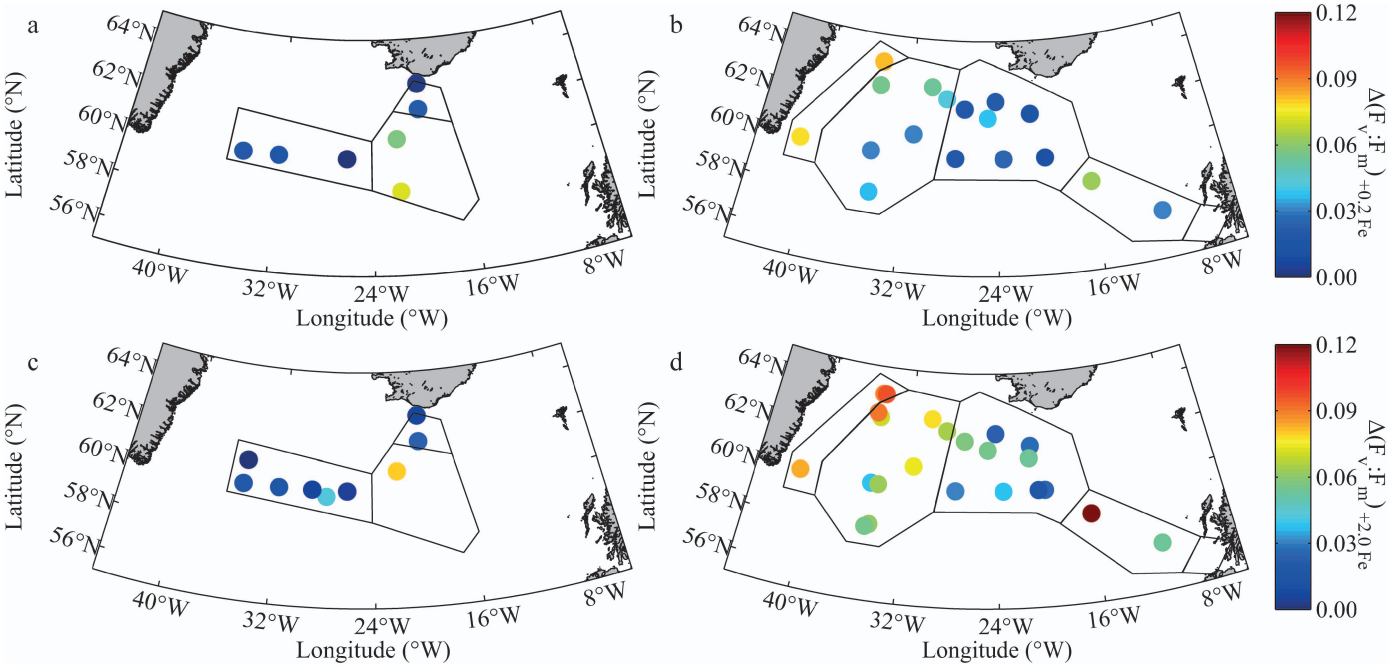

Fig. 5. Experimental values of $\Delta(F_v:F_m)$ calculated after 24 hr for (a,b) the 0.2 nmol L^{-1} iron (+ 0.2 Fe) and (c,d) the 2.0 nmol L^{-1} iron (+ 2.0 Fe) addition treatments during (a,c) the spring and (b,d) summer cruises. Regions are as indicated in Figure 1.

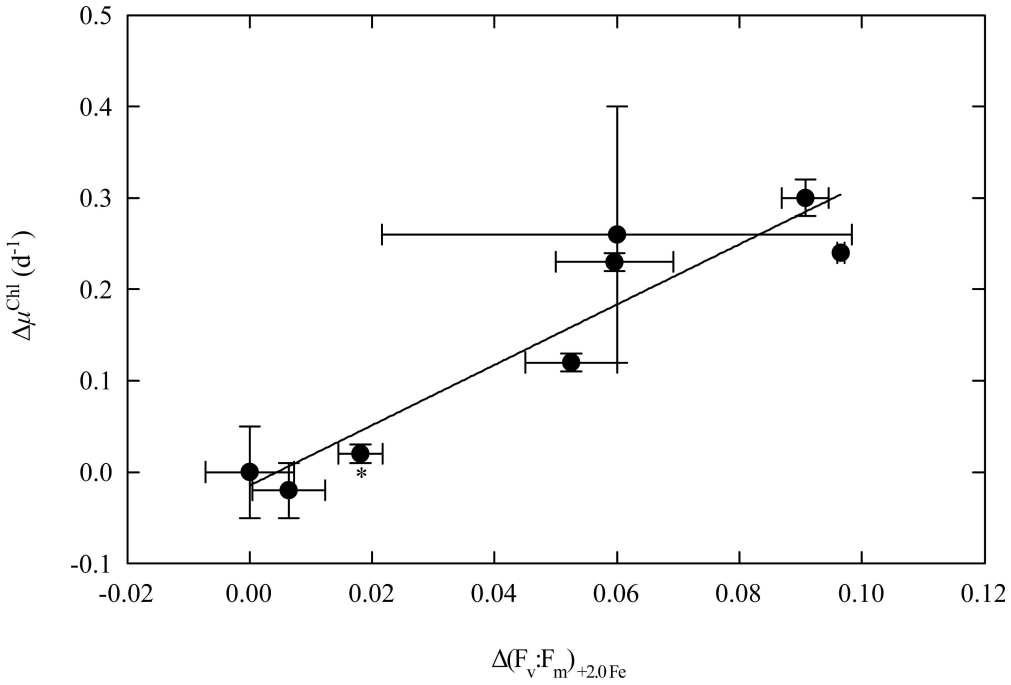

Fig. 6. $\Delta(F_v:F_m)_{+2.0\ Fe}$ plotted against the difference in chlorophyll derived net growth rates over 72 h ($\Delta\mu^{Chl}$ (d^{-1})) for all long-term experiments, where $\Delta\mu^{Chl}$ (d^{-1}) is μ^{Chl} (d^{-1}) for the + Fe treatment minus μ^{Chl} (d^{-1}) from the control treatment. *Growth rate calculated over 48 h only because of shortened experimental duration. Shown are averages with ± standard errors (where $n = 2$ or 3 for $\Delta(F_v:F_m)_{+2.0\ Fe}$ and $n = 3$ or 5 for $\Delta\mu^{Chl}$).

chlorophyll (Fig. 8). Clear spatial differences in bloom timing and progression were observed within the HLNA during 2010. The Iceland basin, Western Irminger Basin, and Rockall region bloomed earlier in the spring (Figs. 1, 2a). However, while there was near complete nutrient drawdown in the Iceland Basin by summer (Fig. 2d), there was incomplete nutrient drawdown (residual nitrate > 1 μmol L^{-1}) in the Western Irminger Basin and Rockall region. In contrast, the Central Irminger Basin bloomed later in the growing season (Figs. 1, 2b) with incomplete nutrient drawdown where the bloom was still underway (Fig. 2d). The almost complete nutrient drawdown observed in the Iceland Basin in the present study is anomalous for this region, with values (< 1 μmol L^{-1} DIN) being lower than typically recorded for the summer period (Sanders et al. 2005; Nielsdóttir et al. 2009), possibly indicative of an additional source of iron to this basin in 2010.

Grow-out bioassay incubation experiments (Fig. 3) demonstrated the development of iron limitation of the in situ phytoplankton population in the Central and Western Irminger Basin from spring to summer but showed evidence of an iron and nitrate colimited system in the Iceland Basin by summer (Table 1; Fig. 3). Size-fractionated analysis of the phytoplankton community in situ and during bioassay experiments suggested that the larger size fraction (> 5 μm) was experiencing greater iron stress and consequently responded more strongly to iron addition (Fig. 7). Such observations are consistent with the similar responses found during an in situ iron release in HNLC systems (Kolber et al. 1994) and suggest that smaller cells might be less susceptible to iron stress when availability is low (Cullen 1991; Price et al. 1994). Community-level characteristics of iron stress development within the HLNA spring bloom thus appear consistent with the hypothesis that iron limitation develops principally through broadly increasing levels of stress for larger cell sizes (Hudson and Morel 1990; Sunda and Huntsman 1997; De Baar et al. 2005). Subsequent iron limitation of macronutrient drawdown may then represent a combined effect of grazer control of the small-celled populations, with restrictions on the growth rates of the larger, less heavily grazed cells, resulting from low iron availability (Cullen 1991; Price et al. 1994; Sunda and Huntsman 1997).

Short duration iron-addition experiments conducted over the growing season enabled us to map the spatial and temporal extent of iron stress throughout the HLNA using the derived variable $\Delta(F_v:F_m)_{+0.2\ Fe\ or\ +2.0\ Fe}$ (Figs. 4, 5). Moreover, the value of $\Delta(F_v:F_m)_{+2.0\ Fe}$ was well correlated with observed differences in net growth rates inferred from chlorophyll accumulation following iron addition in the longer term grow-out experiments (Fig. 6). Such an empirical relationship between $\Delta(F_v:F_m)_{+2.0\ Fe}$ and $\Delta\mu^{Chl}$ should not be taken to infer any universal relationship between the absolute value of $F_v:F_m$ and phytoplankton growth rates (Parkhill et al. 2001; Price 2005; Kruskopf and Flynn 2006). For example, high values of $F_v:F_m$ have been observed under steady-state iron or nitrogen limitation in culture (Parkhill et al. 2001; Price 2005) and nitrogen (iron) (co-)limitation both in laboratory studies (Schrader et al. 2011) and in situ (Behrenfeld et al. 2006). However, the observed correlation between two independent measures of the relative level of iron stress within the studied natural communities (Fig. 6)

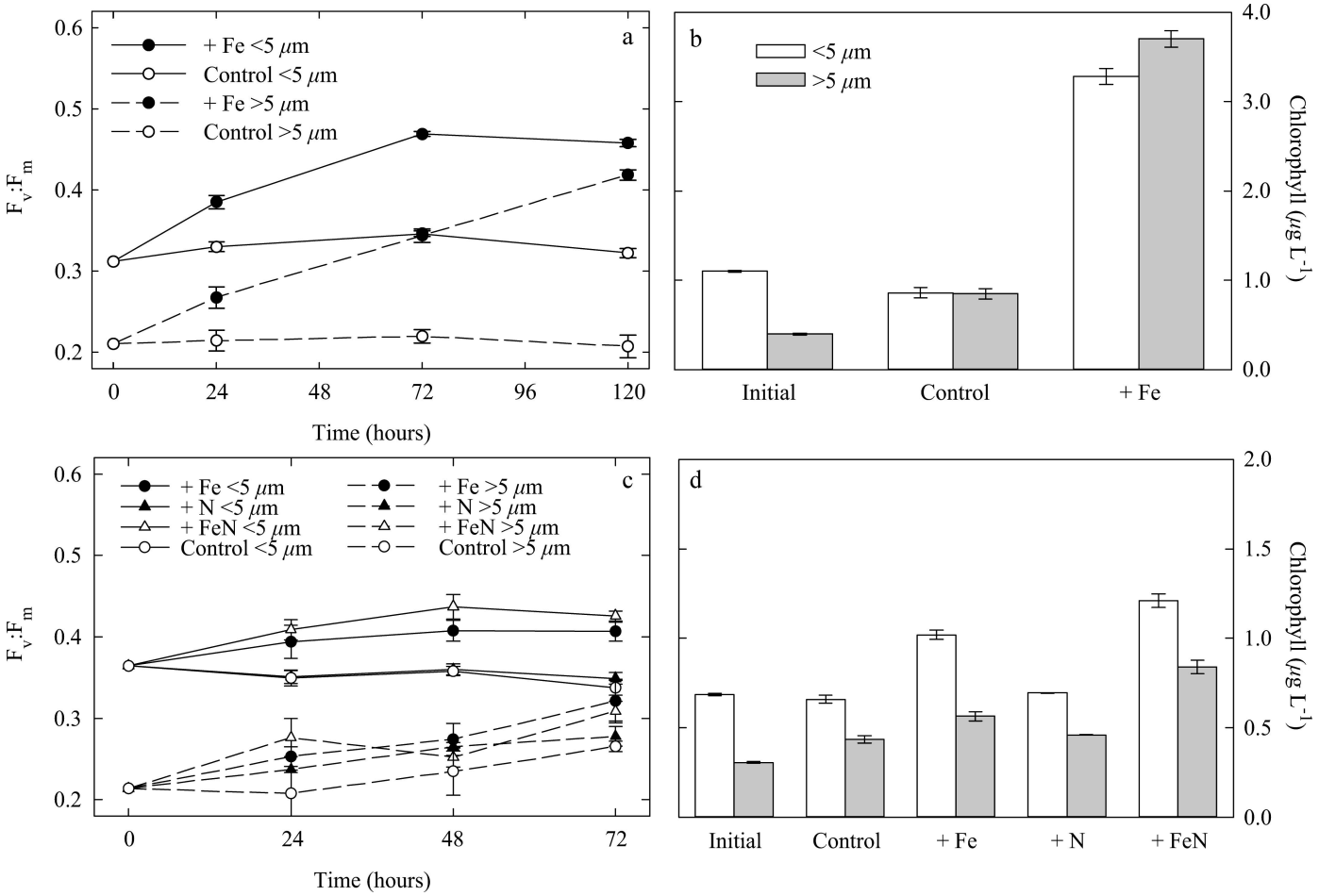

Fig. 7. (a,c) Size-fractionated $F_v : F_m$ and (b,d) chlorophyll responses from long-term (> 24 h) experiments set up in (a,b) the Irminger basin (experiment D354.6) and (c,d) the Iceland basin (experiment D354.7) during the summer. Shown are averages with ± standard errors (n = 3 for all time points of D354.7, and n = 3, 2, 2, and 5 for 0, 24, 72, and 120 h time points in D354.6).

provided empirical evidence that physiological iron stress, as indicated by the short-term response of a biomass-independent measure of phytoplankton physiology ($F_v : F_m$), was likely accompanied by a significant repression of phytoplankton community growth rates.

Placing our experimental results within the seasonal cycle resolved using satellite-derived bloom timing alongside the in situ chlorophyll and DIN concentrations (Fig. 8), the four broad stages representing (A) prebloom, (B) bloom, (C) postbloom high DIN, and (D) postbloom low DIN conditions (as defined in Fig. 2) could be related to differing levels of iron stress (Fig. 8). Low levels of iron stress, which were inferred from measurements of $\Delta(F_v : F_m)$ (Fig. 8b) and $\Delta\mu^{Chl}$ (Fig. 8c), were observed under prebloom conditions (e.g., spring in the Central Irminger Basin), when chlorophyll was low (Fig. 8a), DIN was high (Fig. 8b), and in situ $F_v : F_m$ was high (Fig. 2g). Low levels of iron stress were also observed under postbloom conditions (summer in Iceland Basin) when chlorophyll was low, DIN was depleted, and in situ $F_v : F_m$ was intermediate (Fig. 2h), with long-term grow-out experiments indicating a condition approximating Fe and N colimitation in this system (Fig. 3g,h). Between these two conditions, higher levels of iron stress coincided with the peak of the bloom (Fig. 8a), while the highest levels were observed under postbloom high DIN conditions (Fig. 8b), coincident with the lowest in situ values of $F_v : F_m$ (Fig. 2h). In 2010 such conditions prevailed during summer in the Western side of the Irminger Basin and the Rockall region (Fig. 2d).

Resource availability and loss terms are both crucial determinants of net community growth and hence ultimately biomass accumulation and/or (macro-) nutrient removal (Banse 1991; Banse 2002). Although significant levels of iron stress developed within the HLNA during the peak of the phytoplankton bloom, nitrate removal appeared to continue beyond this stage in some regions (Fig. 8b), indicating that the community retained a capacity for net growth (Fig. 8c). Consequently, although physiological iron stress appears to develop at some stage in the bloom cycle throughout the HLNA (Figs. 5, 8) and is likely linked to restriction of net community growth rates (Fig. 6), with $\mu^{Chl,\ net}$ up to 0.3 d^{-1} higher following the addition of iron (Table 1 and Fig. 8c), the development of iron stress may not necessarily correspond to an ultimate

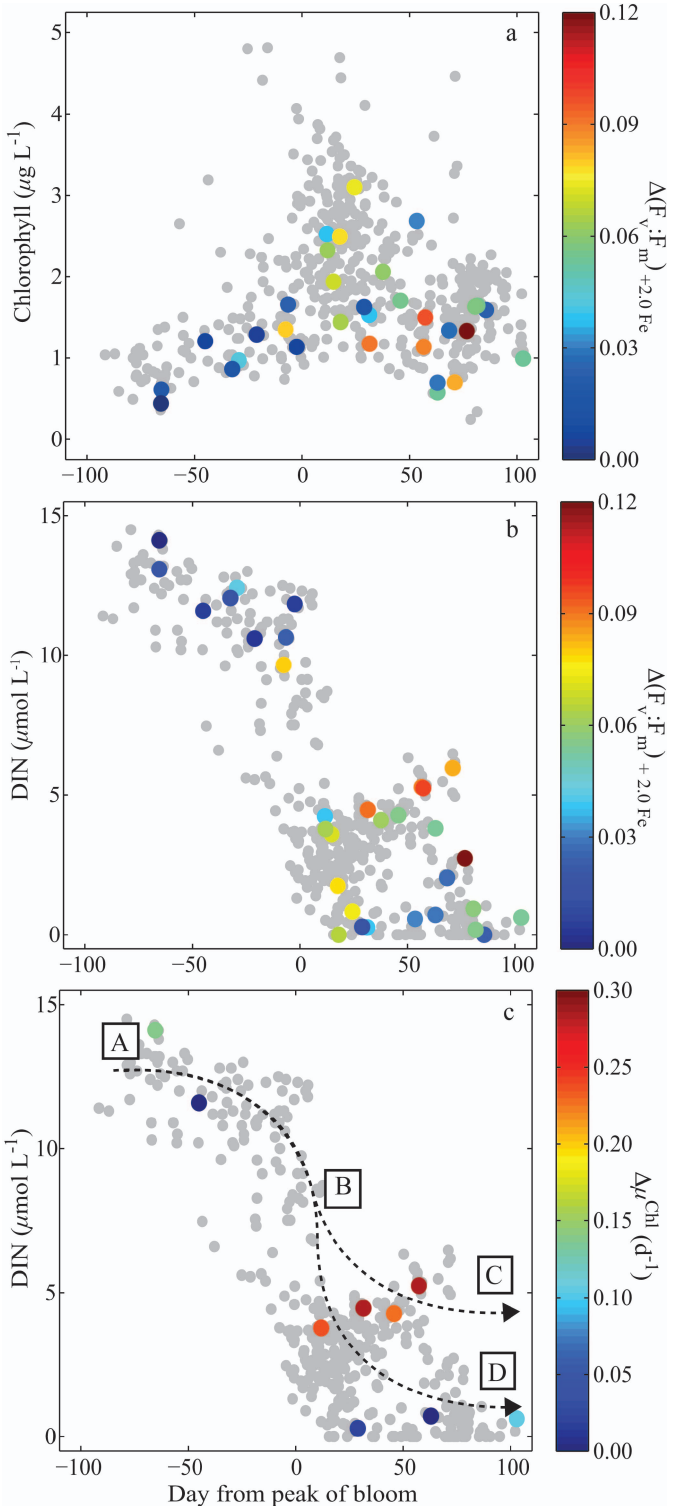

Fig. 8. (a) In situ chlorophyll data (μg L^{-1}) and relative degree of Fe stress ($\Delta(F_v:F_m)_{+2.0\ Fe}$), (b) in situ DIN ($\mu$mol L^{-1}) data and $\Delta(F_v:F_m)_{+2.0\ Fe}$, and (c) in situ DIN and difference in net chlorophyll growth rate following Fe addition ($\Delta\mu^{Chl}$ (d^{-1})) relative to time of peak of bloom. (c) superposed conceptualized model of bloom dynamics, demonstrating two different post-bloom scenarios (low DIN and high DIN) associated with different degrees of Fe stress and iron limited growth rates. Bloom timing as indicated in Fig. 1, with regions associated with different conditions defined as in Fig. 2.

restriction on overall biomass and nutrient drawdown, i.e., Liebig-type limitation (Cullen 1991), in all cases. Indeed, continued net community phytoplankton growth and nutrient drawdown beyond the point where some degree of iron stress develops only requires that any suppression of growth still leaves the gross rate higher than the combined loss terms, including, e.g., grazing (Walsh 1976), sinking (Walsby and Reynolds 1980), and viral lysis (Bratbak et al. 1993).

Although loss rates within long-term grow-out experiments will likely differ from in situ values (Banse 1991), mortality might be expected to be reasonably consistent between controls and nutrient amended treatments, at least over short timescales. Recognizing the additional caveats involved in inferring net phytoplankton growth rates from chlorophyll accumulation due to increases in cellular chlorophyll following relief of iron stress (Geider and La Roche 1994; Moore et al. 2007), the calculated values of $\Delta\mu^{Chl}$ (Fig. 6; Table 1) potentially provide an upper bound on the level of iron limitation of phytoplankton growth rates (Fig. 8c). Maximal phytoplankton growth rates at the in situ temperatures (6–14°C) would likely lie in the range from 1 to 2 d^{-1} (Eppley 1972). However, loss terms will be significant in situ (Banse 2002), and maximal net community growth rates within the bloom are typically < 0.1 d^{-1} (Behrenfeld 2010). Consequently, we suggest that levels of growth rate iron limitation approaching 0.3 d^{-1}, as were suggested by our long-term experiments (Figs. 3, 6; Table 1), would not only be sufficient to significantly influence bloom dynamics, but could also potentially act to terminate the bloom before complete macronutrient removal under some circumstances (Figs. 2d, 8). Such a scenario is entirely consistent with the apparent level of physiological iron stress (Figs. 3, 7) and hence potential growth rate limitation (Fig. 6), being highest under those postbloom conditions where macronutrients remain elevated (Fig. 8).

Our observations of near complete nitrate drawdown in the Iceland Basin (Fig. 2d), in marked contrast to previous observations (Nielsdóttir et al. 2009), alongside incomplete removal of nitrate in the Western Irminger Basin and Rockall regions in the same growing season (Fig. 2d), provide some indication of how finely poised the HLNA system may be between having sufficient or insufficient iron to drive complete macronutrient drawdown. We speculate that both variability in the overall supply ratios of iron and macronutrients (Nielsdóttir et al. 2009) and shifts in community composition between large cells experiencing greater iron stress and smaller cells experiencing lower iron stress (Fig. 7) may interact with group-specific variability in grazing mortality and other loss terms (Cullen 1991; Price et al. 1994) to dictate whether complete surface macronutrient removal occurs over the annual cycle.

We thus propose the following conceptual model for the influence of iron availability on the bloom dynamics of the HLNA (Fig. 8c). Low chlorophyll (Fig. 2a), high DIN (Fig. 2c), high $F_v:F_m$ (Fig. 2g), and a low $\Delta(F_v:F_m)_{+0.2\ Fe\ and\ +2.0\ Fe}$ (Fig. 5a,b) characterize the winter or prebloom condition (labeled A in Figs. 2 and 8), likely representing a nutrient replete, and possibly light-limited, system. As light limitation (Sverdrup 1953) and/or grazing

pressure (Behrenfeld 2010) is reduced, a bloom is initiated. Macronutrients are then consumed as the bloom develops (Fig. 8b, labeled B Fig. 2); however, restricted iron (bio-) availability in the HLNA results in the development of iron stress during the bloom. Ecosystem dynamics (Cullen 1991; Price et al. 1994; Banse 2002) interacting with group-specific susceptibility to iron stress (Fig. 7) may then combine with variable iron supply either interannually, interbasin, or intrabasin (Fig. 5) to dictate whether the macronutrients (e.g., DIN) are completely removed (Figs. 2d; 8b,c). Consequently, the postbloom condition either tends towards complete nitrate removal (labeled D in Fig. 2) and a N-limited or Fe- and N-colimited system (Fig. 3g,h), as observed in the Iceland Basin during 2010, or incomplete nitrate removal (labeled C in Fig. 2) and a Fe-limited system, as observed in the same basin in 2007 (Nielsdóttir et al. 2009) and in the Western Irminger Basin and Rockall region in 2010 (Fig. 3e,f).

The current study represents the first extensive spatial and temporal mapping of the degree of iron stress in a large oceanic region using rapid experimentally induced changes in photophysiology ($\Delta(F_v : F_m)$) placed in the context of the seasonal cycle. The results suggest that the development of iron stress in the HLNA is closely linked to the accumulation of phytoplankton biomass and hence presumably increasing iron requirements, alongside the tendency for cumulative whole community uptake to reduce iron availability. Consequently, in this system, the seasonal progression of the bloom appears to be a crucial control on the development of iron stress, which then plays a significant role in dictating overall macronutrient drawdown. Observed regional contrasts in the degree of iron stress were hence at least partially dictated by variability in the temporal development of the bloom. The North Atlantic clearly differs from the other high-latitude oceanic regions, where a lack of iron contributes to restricted major macronutrient removal, resulting in the HNLC condition. However, even in the highly productive HLNA system, iron availability appears to influence the overall extent of macronutrient removal and hence ultimately both the local strength and efficiency of the biological carbon pump.

Acknowledgments

We thank the captain and crew of the RRS *Discovery* during research cruises D350 and D354, alongside all the scientists involved in both cruises. Particular thanks to Stephanie Henson for initial help with the satellite data. Comments from two anonymous reviews are gratefully acknowledged. This work was supported by the Natural Environment Research Council (UK) through grant NE/E005489/1 to EPA and CMM and a studentship to T.R.K.

References

Arrigo, K. R. 2005. Marine microorganisms and global nutrient cycles. Nature **437:** 349–355, doi:10.1038/nature04159

Banse, K. 1991. Rates of phytoplankton cell devision in the field and in iron enrichment experiments. Limnol. Oceanogr. **36:** 1886–1898, doi:10.4319/lo.1991.36.8.1886

———. 2002. Steemann Nielsen and the zooplankton. Hydrobiologia **480:** 15–28, doi:10.1023/A:1021220714899

Behrenfeld, M. J. 2010. Abandoning Sverdrup's critical depth hypothesis on phytoplankton blooms. Ecology **91:** 977–989, doi:10.1890/09-1207.1

———, K. Worthington, R. M. Sherrell, F. P. Chavez, P. Strutton, M. Mcphaden, and D. M. Shea. 2006. Controls on tropical Pacific Ocean productivity revealed through nutrient stress diagnostics. Nature **442:** 1025–1028, doi:10.1038/nature05083

Boyd, P. W. 2002. Environmental factors controlling phytoplankton processes in the Southern Ocean. J. Phycol. **38:** 844–861, doi:10.1046/j.1529-8817.2002.t01-1-01203.x

———, and E. R. Abraham. 2001. Iron-mediated changes in phytoplankton photosynthetic competence during SOIREE. Deep-Sea Res. II **48:** 2529–2550, doi:10.1016/S0967-0645(01)00007-8

———, and others. 2007. Mesoscale iron enrichment experiments 1993–2005: Synthesis and future directions. Science **315:** 612–617, doi:10.1126/science.1131669

Bratbak, G., J. K. Egge, and M. Heldal. 1993. Viral mortality of the marine alga *Emiliania Huxleyi* (Haptophyceae) and termination of algal blooms. Mar. Ecol. Prog. Ser. **93:** 39–48, doi:10.3354/meps093039

Cullen, J. J. 1991. Hypotheses to explain high-nutrient conditions in the open sea. Limnol. Oceanogr. **36:** 1578–1599, doi:10.4319/lo.1991.36.8.1578

———, and R. F. Davis. 2003. The blank can make a big difference in oceanographic measurements. Limnol. Oceanogr. Bull. **12:** 29–35.

De Baar, H. J. W., A. G. J. Buma, R. F. Nolting, G. C. Cadee, G. Jacques, and P. J. Treguer. 1990. On iron limitation of the Southern Ocean: Experimental observations in the Weddell and Scotia Seas. Mar. Ecol. Prog. Ser. **65:** 105–122, doi:10.3354/meps065105

———, and others. 2005. Synthesis of iron fertilization experiments: From the iron age in the age of enlightenment. J. Geophys. Res. C Oceans **110:** C09S16, doi:10.1029/2004JC002601

Eppley, R. W. 1972. Temperature and phytoplankton growth in the sea. Fish. Bull. **70:** 1063–1085.

Geider, R. J., and J. La Roche. 1994. The role of iron in phytoplankton photosynthesis, and the potential for iron-limitation of primary productivity in the sea. Photosynth. Res. **39:** 275–301, doi:10.1007/BF00014588

Greene, R. M., Z. S. Kolber, D. G. Swift, N. W. Tindale, and P. G. Falkowski. 1994. Physiological limitation of phytoplankton photosynthesis in the eastern equatorial Pacific determined from variability in the quantum yield of fluorescence. Limnol. Oceanogr. **39:** 1061–1074, doi:10.4319/lo.1994.39.5.1061

Henson, S. A., R. Sanders, C. Holeton, and J. T. Allen. 2006. Timing of nutrient depletion, diatom dominance and a lower-boundary estimate of export production for Irminger Basin, North Atlantic. Mar. Ecol. Prog. Ser. **313:** 73–84, doi:10.3354/meps313073

Hudson, R. J. M., and F. M. M. Morel. 1990. Iron transport in marine-phytoplankton—kinetics of cellular and medium coordination reactions. Limnol. Oceanogr. **35:** 1002–1020, doi:10.4319/lo.1990.35.5.1002

Jickells, T. D., and others. 2005. Global iron connection between desert dust, ocean biogeochemistry, and climate. Science **308:** 67–71, doi:10.1126/science.1105959

Kolber, Z. S., R. T. Barber, K. H. Coale, S. E. Fitzwater, R. M. Greene, K. S. Johnson, S. Lindley, and P. G. Falkowski. 1994. Iron limitation of phytoplankton photosynthesis in the Equatorial Pacific-Ocean. Nature **371:** 145–149, doi:10.1038/371145a0

Kruskopf, M., and K. J. Flynn. 2006. Chlorophyll content and fluorescence responses cannot be used to gauge reliably phytoplankton biomass, nutrient status or growth rate. New Phytol. **169:** 525–536, doi:10.1111/j.1469-8137.2005.01601.x

Laws, E. A., P. G. Falkowski, W. O. Smith Jr., H. Ducklow, and J. J. Mccarthy. 2000. Temperature effects on export production in the open ocean. Global Biogeochem. Cycles **14:** 1231–1246, doi:10.1029/1999GB001229

Martin, J. H., and S. E. Fitzwater. 1988. Iron deficiency limits phytoplankton growth in the northeast Pacific subarctic. Nature **331:** 341–343, doi:10.1038/331341a0

———, ———, R. M. Gordon, C. N. Hunter, and S. J. Tanner. 1993. Iron, primary production and carbon nitrogen flux studies during the JGOFS North Atlantic bloom experiment. Deep-Sea Res. II **40:** 115–134, doi:10.1016/0967-0645(93)90009-C

Measures, C. I., W. M. Landing, M. T. Brown, and C. S. Buck. 2008. High-resolution Al and Fe data from the Atlantic Ocean CLIVAR-CO(2) repeat hydrography A16N transect: Extensive linkages between atmospheric dust and upper ocean geochemistry. Global Biogeochem. Cycles **22:** GB1005, doi:10.1029/2007GB003042

Milne, A., W. Landing, M. Bizimis, and P. Morton. 2010. Determination of Mn, Fe, Co, Ni, Cu, Zn, Cd and Pb in seawater using high resolution magnetic sector inductively coupled mass spectrometry (HR-ICP-MS). Anal. Chim. Acta **665:** 200–207, doi:10.1016/j.aca.2010.03.027

Moore, C. M., M. M. Mills, A. Milne, R. Langlois, E. P. Achterberg, K. Lochte, R. J. Geider, and J. La Roche. 2006. Iron limits primary productivity during spring bloom development in the central North Atlantic. Global Change Biol. **12:** 626–634, doi:10.1111/j.1365-2486.2006.01122.x

———, S. Seeyave, A. E. Hickman, J. T. Allen, M. I. Lucas, H. Planquette, R. T. Pollard, and A. J. Poulton. 2007. Iron-light interactions during the CROZet natural iron bloom and EXport experiment (CROZEX) I: Phytoplankton growth and photophysiology. Deep-Sea Res. II **54:** 2045–2065, doi:10.1016/j.dsr2.2007.06.011

Nielsdóttir, M. C., C. M. Moore, R. Sanders, D. J. Hinz, and E. P. Achterberg. 2009. Iron limitation of the postbloom phytoplankton communities in the Iceland Basin. Global Biogeochem. Cycles **23:** 1–13, doi:10.1029/2008GB003410

Parkhill, J., G. Maillet, and J. J. Cullen. 2001. Fluorescence-based maximal quantum yield for PSII as a diagnostic of nutrient stress. J. Phycol. **37:** 517–529, doi:10.1046/j.1529-8817.2001.037004517.x

Price, N. M. 2005. The elemental stoichiometry and composition of an iron-limited diatom. Limnol. Oceanogr. **50:** 1149–1158, doi:10.4319/lo.2005.50.4.1159

———, B. A. Ahner, and F. M. M. Morel. 1994. The Equatorial Pacific-Ocean—grazer-controlled phytoplankton populations in an iron-limited ecosystem. Limnol. Oceanogr. **39:** 520–534, doi:10.4319/lo.1994.39.3.0520

Prospero, J. M., J. E. Bullard, and R. Hodgkins. 2012. High-latitude dust over the North Atlantic: Inputs from Icelandic proglacial dust storms. Science **335:** 1078–1082, doi:10.1126/science.1217447

Saito, M. A., T. J. Goepfert, and J. T. Ritt. 2008. Some thoughts on the concept of colimitation: Three definitions and the importance of bioavailability. Limnol. Oceanogr. **53:** 276–290, doi:10.4319/lo.2008.53.1.0276

Sanders, R., S. Brown, S. A. Henson, and M. I. Lucas. 2005. New production in the Irminger basin during 2002. J. Mar. Syst. **55:** 291–310, doi:10.1016/j.jmarsys.2004.09.002

———, and T. Jickells. 2000. Total organic nutrients in Drake Passage. Deep-Sea Res. I **47:** 997–1014, doi:10.1016/S0967-0637(99)00079-5

Schrader, P. S., A. J. Milligan, and M. J. Behrenfeld. 2011. Surplus photosynthetic antenna complexes underlie diagnostics of iron limitation in a cyanobacterium. PLoS ONE **6:** e18753, doi:10.1371/journal.pone.0018753

Siegel, D. A., S. C. Doney, and J. A. Yoder. 2002. The North Atlantic spring phytoplankton bloom and Sverdrup's critical depth hypothesis. Science **296:** 730–733, doi:10.1126/science.1069174

Suggett, D. J., C. M. Moore, A. E. Hickman, and R. J. Geider. 2009. Interpretation of fast repetition rate (FRR) fluorescence: Signatures of phytoplankton community structure versus physiological state. Mar. Ecol. Prog. Ser. **376:** 1–19, doi:10.3354/meps07830

Sunda, W. G., and S. A. Huntsman. 1997. Interrelated influence of iron, light and cell size on marine phytoplankton growth. Nature **390:** 389–392, doi:10.1038/37093

Sverdrup, H. U. 1953. On conditions for the vernal blooming of phytoplankton. J. Cons. Int. Explor. Mer **18:** 287–295.

Volk, T., and M. I. Hoffert. 1985. Ocean carbon pumps: Analysis of relative strengths and efficiencies in ocean-driven atmospheric CO_2, p. 99–110. *In* E. T. Sundquist and W. S. Broecker [eds.], The carbon cycle and atmospheric CO_2: Natural varations Archean to Present. AGU.

Walsby, A. E., and C. S. Reynolds. 1980. Sinking and floating, p. 371–412. *In* I. Morris [ed.], The physiological ecology of phytoplankton. Studies in Ecology. Blackwell.

Walsh, J. J. 1976. Herbivory as a factor in patterns of nutrient utilization in the sea. Limnol. Oceanogr. **21:** 1–13, doi:10.4319/lo.1976.21.1.0001

Welschmeyer, N. A. 1994. Fluorometric analysis of chlorophyll-*a* in the presence of chlorophyll-b and pheopigments. Limnol. Oceanogr. **39:** 1985–1992, doi:10.4319/lo.1994.39.8.1985

Associate editor: Robert R. Bidigare

Received: 26 June 2012
Accepted: 05 November 2012
Amended: 20 November 2012